PHYSICAL REVIEW B VOLUME 8, NUMBER 6 15 SEPTEMBER 1973

Influence of Boundary Conditions and of Electronic and Vibrational Surface Phenomena on Low-Energy-Electron Diffraction from the Low-Index Faces of Aluminum

C. B. Duke, N. O. Lipari, and U. Landman
Xerox Research Laboratories, Rochester, New York 14644
(Received 27 November 1972)

An overlapping-atomic-charge-density model is used to construct muffin-tin potentials of surface ion cores on the (100), (110), and (111) faces of aluminum. When applied to bulk ion cores, this model leads to potentials whose associated elastic-low-energy electron diffraction (ELEED) intensities are indistinguishable from those predicted by a "correct" self-consistent muffin-tin potential. Moreover, the alterations in the ELEED intensities wrought by the differences between the surface and bulk potentials are small relative to those caused by plausible variations of the vacuum-solid boundary conditions among those commonly used by the various theoretical groups specializing in intensity calculations. The enhanced vibrations of the surface ion cores relative to those in the bulk, however, can lead to substantial changes in the ELEED intensities at fixed temperature as well as in the temperature dependence of these intensities. When their consequences are incorporated into the model, excellent correspondence with experimental ELEED spectra on Al(111) is achieved, but the comparable correspondence for Al(100) is poor. The absolute intensities of ELEED spectra from a planar Al(100) surface can be described by the model only if surface-plasmon loss processes are regarded as extending the inelastic collision damping about one lattice spacing in front of the outermost layer of ion cores.

I. INTRODUCTION

It is widely believed, as may be discerned from inspection of any recent review of the topic, [1–5] that the major application anticipated for elastic low-energy-electron diffraction (ELEED) is the determination of the geometrical structure of the outermost few layers of a crystalline solid. For this application to be realized, however, requires a precisely specified knowledge of the other aspects of the electron-solid force law so that uncertainties in, say, the electron–ion-core scattering factors can be separated from those in the positions of the scatterers. This requirement, in turn, has appeared to become more critical as various workers[6–8] have recognized that only the top few layers of the solid contribute to the observed ELEED intensities and, indeed, the electronic and vibrational properties of these layers can differ significantly from those in the "bulk" of the solid. [9]

In contrast to this expectation of surface sensitivity, however, a wide variety of studies[5,7,8,10–15] have revealed that for the close-packed faces of several metals (especially aluminum and copper), calculations using various bulk band-structure potentials and adjustable complex one-electron optical (or "inner") potentials provide comparable and quite tolerable descriptions of observed *"isothermal"* room-temperature ELEED intensities. This result is perhaps surprising in light of the early, almost universal, anticipation[11,15–18] that the method of evaluating the electron–ion-core potentials was likely to exert a strong influence on the resulting ELEED intensities. Because of the importance of this topic in separating electronic from geometrical effects in the case of adsorbed monolayers, [5,19,20] we decided to extend previous analyses[5–8,10–12,15,16,21,22] of ELEED from the low-index faces of aluminum in order to examine this separation in a case which has been studied, both experimentally and theoretically, by several groups in different laboratories.

We focus our attention on four central issues.

(i) Given that differing boundary conditions, methods of calculation, and potentials have been used in calculating ELEED intensities from aluminum, we first assess the effect of each of these individually on the ensuing model predictions.

(ii) Having discovered in (i) that a simple model of overlapping charge densities yields ELEED intensities essentially indistinguishable from those of a properly self-consistent potential, we use this model to calculate the altered surface electron–ion-core potentials (due to different atomic coordination) at the (100), (110), and (111) surfaces of aluminum. We show that despite substantial changes in potential, the predicted ELEED intensities remain almost unaffected by these "electronic" surface effects. Although earlier analyses have been given[5,6,16,22] of the consequences of differing bulk and surface electron–ion-core scattering factors, the present analysis is the first to incorporate a calculation of the changes in these scattering factors using a plausible microscopic model which is demonstrated to be adequate in the case of "bulk" ion cores.

(iii) Recognizing that the electronic inequivalence of the surface and bulk scatterers is of minor significance in these calculations of ELEED intensities, we then examine the importance of their vi-

brational inequivalence. The consequences of the enhanced vibrational amplitudes of surface scatterers can be quite striking, especially in that this phenomenon preferentially obliterates the smaller (or "secondary") peaks in the scattered intensity relative to the prominent ones. An important subsidiary issue arises in this context which we are not able to resolve completely: the compatibility of models constructed to describe the temperature dependence of prominent peaks in the ELEED intensities[23] with those which are utilized to analyze alterations in these intensities with changing beam parameters at fixed temperature.[7,8,10–17]

(iv) Finally we examine, for the first time, the quantitative question of the prediction of the absolute magnitude of ELEED intensities from aluminum by the theoretical models. Burkstrand's data[24] on Al(100) indicate that straigntforward versions of the model, including surface vibrational effects and using large damping, lead to predicted intensities almost an order of magnitude larger than those observed. Only the extension of the optical potential several angstroms outside the ion cores (as could be due, e.g., to surface-plasmon creation by the incident electron[25]) or the assumption of planar scattering areas much smaller than the diameter of the incident electron beam can explain this puzzle.

We proceed in five steps. In Sec. II we review the parameters which specify our model electron-solid interaction and examine the ELEED intensities predicted using various boundary conditions in Sec. III. Then we turn our attention to the consequences of surface electronic and vibrational phenomena in Secs. IV and V, respectively. The question of absolute intensities is discussed in Sec. VI and a synopsis of our results is given in Sec. VII.

II. MODEL PARAMETERS

Since the computational procedure used in our analysis already has been described by Laramore and Duke,[7] we confine our discussion of the model to a recapitulation of the definition of its parameters. Three types of these parameters occur: those describing the electron–ion-core potential in a rigid lattice, those describing the electron-electron–interaction-induced "optical" potential, and those describing the thermal motions of the ion cores. We discuss each in turn.

The electron–ion-core interaction in a rigid lattice is described by a one-electron muffin-tin potential. Specifically, we consider a model consisting of spherically symmetrical ion-core potentials within individual layers of the solid parallel to the surface.[26–28] For such potentials, the scattering of the electrons from an individual ion core is specified by a sequence of phase shifts $\{\delta_l(E)\}$, which depend on the angular momentum $L = l\hbar$ and energy E of the incident electron relative to the scatterer. All electron–ion-core interaction potentials were characterized by evaluating the phase shifts for $l \leq 4$ and energies in the range $0 \leq E \leq 180$ eV by numerical integration of the Schrödinger equations associated with the individual ion cores. In our evlauation of the ELEED intensities, however, only the first three phase shifts, $l \leq 2$, were used,[7,23] thereby limiting the quantitative validity of our analysis to energies $E \leq 80$ eV.

The ion-core potentials themselves were evaluated using an overlapping-atomic-charge-density model and compared at various stages of the calculation with the self-consistent potential obtained by Snow[29] as applied to the analysis of ELEED intensities by Marcus, Jepsen, and Jona.[8,11,15] We proceed in two steps. First, the crystal potential $V_c(r)$ is calculated, and then it is reduced to the muffin-tin form for evaluation of the phase shifts. The crystal potential is calculated using the expression[30]

$$V_c(r) = -\frac{Ze^2}{r} + \frac{e^2}{r}\int_0^r \sigma(t)dt - e^2\int_r^\infty \frac{\sigma(t)}{t}\,dt - 3e^2\left(\frac{3\sigma(r)}{32\pi^2 r^2}\right)^{1/3} \quad (1)$$

in which $\sigma(r)$ is the electronic radial number density at a distance r from an ion core at $r = 0$. The last term in Eq. (1) is the Slater approximation[31] to the exchange energy. The symbol Z designates the atomic number and e is the elemental electronic charge. Our overlapping-atomic-charge-density model is defined by the use of a crystal charge density, $\sigma(\vec{r})$, at a given point $\vec{r}$ which is the superposition of atomic charge densities of the constituents of the crystal, i.e.,

$$\sigma(\vec{r}) = \sum_n \sigma_{\text{atomic}}(\vec{r} - \vec{R}_n)\ . \quad (2)$$

The atomic charge densities $\sigma_{\text{atomic}}(\vec{r})$, are calculated using a computer program essentially identical to that of Herman and Skillman.[30] Only the spherically symmetric component of the crystal charge density at a given site was used in Eq. (1), and this component was evaluated using Löwdin's α-function expansion[32] as described by Mattheiss.[33] The expansion over lattice sites in Eq. (2) was carried out over the three nearest shells of neighbors of a given ion core.

Once the crystal potential in a given Wigner-Seitz call has been obtained, however, we still must reduce it to muffin-tin form in order to achieve the spherical symmetry required for the calculation of the electron scattering phase shifts. We take the radius of the muffin-tin spheres to be one-half of the nearest-neighbor distance, $r_M = 2.7$ a.u. $= 1.4284$ Å. The value of the constant potential in

between these spheres was selected in one of two ways. In the first, leading to the potential which we label by 1, it was chosen to equal Snow's ("uncorrected") value[29] (i.e., -0.831054 Ry) everywhere. This choice leads to core potentials which depend explicitly on the layer index for the uppermost three layers of the low-index faces of aluminum because of the differing coordination of the ion cores in these layers. Moreover, the "bulk" potential obtained in this fashion differs from Snow's self-consistent potential essentially by only an additive constant. In our overlapping-atomic-charge-density model, however, the average potential in between, as well as within, the muffin-tin spheres depends on the layer index in the upper three layers of the crystal, decreasing in magnitude as the surface is approached. This fact motivated our second choice of the values of the muffin-tin constants, leading to the potential labeled by 2. In this case the constant potential(s) in between the muffin tins in a given layer were taken to equal the average value of the atomic potential in this region for each different atomic layer parallel to the surface. As in the first method, this choice gives rise to discontinuities in the potential at the muffin-tin radius which depend explicitly on the layer index. In the ultimate application of this potential to evaluate ELEED intensities, these discontinuities but not the change in average potential from one layer to the next were incorporated into the model potential. Evidently, the core potentials are the same in both models. Their appreciable change as the surface of the solid is approached is given in Table I for the case of Al(111) which we shall study extensively in Sec. III. As can be seen from the table, for this face the potentials in the second and third layers are almost identical. Such is not the case for either Al(100) or Al(110), both of which also were analyzed using our model. The potentials for Al(100)(used to evaluate the intensities which will be shown later in Figs. 1, 2, 5, 8, and 10) are tabulated in Table II.

TABLE I. Tabulation of surface layer (V_1), second layer (V_2), and bulk (V_B) core potentials for Al (111) predicted by the overlapping-atomic-charge-density model. ($r_M = 2.7$ a.u.) Energies are given in Ry and distances in a.u. The muffin-tin potential obtained using method 2 is indicated as V_0.

r	$-V_1(r)$	$-V_2(r)$	$-V_B(r)$
0.1	203.17	203.20	203.20
0.3	44.90	44.92	44.92
0.5	19.52	19.55	19.55
0.7	10.78	10.81	10.81
0.9	6.813	6.845	6.845
1.1	4.677	4.713	4.713
1.3	3.443	3.485	3.485
1.5	2.705	2.754	2.754
1.7	2.229	2.285	2.285
1.9	1.897	1.961	1.961
2.1	1.655	1.728	1.728
2.3	1.477	1.562	1.562
2.5	1.351	1.449	1.450
2.7	1.267	1.381	1.382
	$-V_0^{(2)} = 1.232$	$-V_0^{(2)} = 1.359$	$-V_0^{(2)} = 1.360$

The most significant feature of the changes in the potentials of the surface ion cores is their increase with increasing values of r, reaching a maximum $\Delta V \sim 2$ eV at the muffin-tin radius. This spatial behavior is caused by the valence electrons responding to alterations in atomic coordination. As one might expect, it leads to the consequence that predominantly the low-partial-wave ($l \leq 1$), low-energy ($E \lesssim 50$ eV), and electron–ion-core phase shifts are influenced by the atomic coordination. This fact, implies, however, that our three partial-wave calculation of ELEED intensities is quite adequate for the discussion of electronic surface effects because for $E \lesssim 50$ eV the $l = 3$ phase shifts are small relative to those for $l \leq 2$.

We next turn to our discussion of the second type of parameters, those associated with the electron-electron–interaction-induced optical potential. In Ref. 7 they are specified by taking the single-electron proper self-energy to assume the form

$$\Sigma(E) = -V_0 - i\hbar[2m(E+V_0)]^{1/2}/m\lambda_{ee}\,, \tag{3}$$

in which V_0 is the real "inner potential" and λ_{ee} is the inelastic-collision damping length. Since one of our interests here is comparing various model calculations, however, we also shall use the form

$$\Sigma(E) = -V_1 - iV_2\,, \tag{4a}$$

in which V_1 and V_2 are real energy-independent constants. This form for the proper self-energy renders our analysis roughly comparable to the "no-reflection matching" boundary condition employed by Jepsen *et al.*,[11,15] provided that after calculating the intensities, we shift all energy scales by an energy Δ defined by

$$V_1 + \Delta/\cos^2\theta = V_0 \tag{4b}$$

for a beam with incident polar angle θ. The inelastic-collision-model computer program treats $k_{\parallel} = (2mE/\hbar^2)^{1/2}\sin\theta$ and E as the independent variables. Consequently, the use of a finite value of Δ in Eq. (4b) changes only the value of momentum normal to the surface $k_\perp^{(0)} = (2mE/\hbar^2)^{1/2}\cos\theta$ to $k_\perp = [2m(E + V_0/\cos^2\theta)/\hbar^2]^{1/2}\cos\theta$. As a result, the incident electron beam is refracted toward the surface normal in such a fashion that its effective angle of incidence is given by $\theta_{eff} = \tan^{-1}[\tan\theta/(1 + V_0/E\cos^2\theta)^{1/2}]$. The use of this value of the angle of incidence and a corresponding Snell's Law refraction for the exit angle, however, is just the

no-reflecting matching boundary condition of Jepsen *et al.* Therefore for the specular beam their utilization of this boundary condition with an inner potential Δ corresponds to our use of $V_1 = 0$ and $\Delta = V_0/\cos^2\theta$.

The final parameters which we must specify are those associated with the vibrational motion of the atomic scatterers. This motion is incorporated into the calculation of the ELEED intensities by a renormalization of the rigid-lattice electron–ion-core vertex. In the case of a rigid lattice, these vertices are given by

$$t_\nu(\vec{k}', \vec{k}) = \frac{4\pi^2 i\hbar^2}{mk(E)} \sum_{l,m} (2l+1)(e^{2i\delta_l^\nu(E)} - 1) \times Y_{lm}^*(\hat{k}') Y_{lm}(\hat{k}), \tag{5a}$$

$$k^2(E) = 2m[E - \Sigma(E)]/\hbar^2 . \tag{5b}$$

The index ν labels the layer parallel to the surface in which the ion core is found. The $\delta_l^\nu(E)$ depend explicitly on this index for $\nu \leq 3$. The consequences of the atomic vibrations of the lattice are introduced, in an approximate way,[27] by the multiplication of the rigid-lattice t vertices by the associated Debye-Waller factor. Using the spherical Debye model of the lattice-vibration spectra we get

$$b_\nu(\vec{k}', \vec{k}) = t_\nu(\vec{k}', \vec{k}) e^{-(\vec{k}' - \vec{k})^2 W_\nu(T)} , \tag{6a}$$

$$W_\nu(T) = \frac{3\hbar^2}{2M_\nu \kappa \Theta_D^\nu} \left[\frac{1}{4} + \left(\frac{T}{\Theta_D^\nu} \right)^2 \int_0^{\Theta_D^\nu / T} \frac{x\,dx}{e^x - 1} \right] \tag{6b}$$

in which M_ν is the mass of the atoms in the layer labeled by ν, Θ_D^ν is the Debye temperature describing the motion of the atoms in this layer,[34] T is the temperature, and κ is the Boltzmann's constant. The quantity $b_\nu(\vec{k}', \vec{k})$ is the renormalized electron–ion-core vertex which is expanded into three partial-wave components ($l \leq 2$) in our calculations of ELEED intensities. For incident beam energies $E \gtrsim 80$ eV it would seem advisable[23] to have higher partial-wave components because both the t_ν vertex and the Debye-Waller factor have appreciable components for $l > 2$. We expect, however, our analysis to be qualitatively correct even though it may overestimate the reduction in the calculated intensities with increasing temperature.[23–27] [It is a slight extension of Laramore's[23] calculations in that three partial waves in the Debye-Waller factor are included in the expansion of $b_\nu(\vec{k}', \vec{k})$.]

A variety of values for the bulk atomic Debye temperature have been used in the literature. Laramore and Duke[7] use $\Theta_D = 426$ °K, Jepsen *et al.*[11,15] employ $\Theta_D = 418$ °K, and Laramore[23] utilizes $\Theta_D = 380$ °K in accord with the most recent x-ray and heat-capacity data.[35] For practical purposes these three values are equivalent, and which we use in a given case depends upon whose work with which we wish to compare our calculations.

The only estimate of a surface Debye temperature of aluminum is that of Laramore.[23] By analyzing the data of Quinto *et al.*,[36] using a model in which only the surface Θ_D differed from that of the bulk ($\Theta_D^{\nu>2} = 380$ °K), he obtained $\Theta_D^1 \cong 180$ °K for the (100) face of aluminum. We shall use his results to illustrate the consequences of the enhanced surfact-ion-core vibrations for this face (See Secs. V and VI.)

III. BOUNDARY CONDITIONS AND COMPUTATIONAL METHODS

As noted in the Introduction, a variety of mathematical models and computational procedures have been used to calculate the ELEED intensities from the low-index surfaces of clean metals. Consequently, it seemed appropriate to initiate our study of surface effects by examining the extent to which the predictions of the various models can be expected to vary because of those features of the models which are unrelated to surface phenomena *per se* but which must be defined in order to perform the calculations and for which different workers have used different definitions. This examination provides an estimate of the intrinsic discrepancies between the various model ELEED intensities which may be regarded as constituting a theoretical "background" uncertainty in these intensities. This uncertainty must be exceeded by the consequences of surface phenomena before these phenomena can be regarded as being of major significance in current analyses of ELEED. We proceed by illustrating the consequences of various models of the bulk electron–ion-core potential, and those of different surface-boundary conditions. This section is con-

TABLE II. Tabulation of the surface layer (V_1), second layer (V_2), and bulk (V_B) core potentials for Al(100) predicted by the overlapping-atomic-charge-density model. ($r_M = 2.7$ a.u.) Energies are given in Ry and distances in a.u. The muffin-tin potential obtained using method 2 is indicated as V_0.

r	$-V_1(r)$	$-V_2(r)$	$-V_B(r)$
0.1	203.16	203.20	203.20
0.3	44.89	44.92	44.92
0.5	19.51	19.55	19.55
0.7	10.78	10.81	10.81
0.9	6.805	6.844	6.845
1.1	4.667	4.712	4.713
1.3	3.432	3.484	3.485
1.5	2.692	2.752	2.754
1.7	2.214	2.283	2.285
1.9	1.880	1.959	1.961
2.1	1.635	1.726	1.728
2.3	1.454	1.560	1.562
2.5	1.323	1.447	1.450
2.7	1.235	1.379	1.382
	$-V_0^{(2)} = 1.196$	$-V_0^{(2)} = 1.357$	$-V_0^{(2)} = 1.360$

cluded with an explicit comparison of our calculations with those of Jepsen *et al.*[11,15]

Turning to our first topic, we recall[7,11] that since in the inelastic collision model the values of k are complex, strictly speaking the $Y_{lm}(\hat{k})$ in expressions like Eq. (5a) are not defined. In both Refs. 7 and 11 this issue was resolved by writing the Y_{lm} as functions of $k_\perp$, $k_\parallel$, and $k(E)$, and explicitly defining the $Y_{lm}(\hat{k})$ by these expressions taking $k(E)$ to be complex as determined by Eq. (5b) and $k_\perp(\vec{g}, E)$ as defined by the conservation of energy and the component of momentum parallel to the surface, i.e.,[7]

$$k_\perp^2(\vec{g}, E) = 2m[E - \Sigma(E)]/\hbar^2 - (\vec{k}_\parallel + \vec{g})^2 , \tag{7a}$$

$$k_\parallel^2 = 2mE \sin^2\theta/\hbar^2 , \tag{7b}$$

Several alternative definitions of $Y_{lm}^*(\hat{k}')$ in terms of the complex perpendicular momentum of the exiting beam have been proposed. Realizing that the exiting beam propagates in the $z < 0$ direction, $-k_\perp(\vec{g}, E)$ was employed by Laramore and Duke.[7] On the other hand, requiring that all complex wave numbers k must lie in the upper half k plane[38] would result in the use of $-\bar{k}_\perp(\vec{g}, E)$. The consequences of the two choices are illustrated in Fig. 1. The intensity profile labeled "Snow-1" is computed using the first form $-k_\perp(\vec{g}, E)$ and that labeled "Snow-2" was computed using $-\bar{k}_\perp(\vec{g}, E)$. Evidently in the second version the intensities at lower energies (i.e., $E \lesssim 50$ eV) change slightly, although their qualitative features remain unaltered. The changes on Al(111) proved much more substantial, however, and included the obliteration of an (observed) peak at $E \cong 15$ eV in the intensity profile of the (00) beam. Moreover, the external beam $Y_{lm}(\hat{k})$ are inserted into the theory by definition, for dissipative electron propagation inside the solid (i.e., they supplant the ordinary joining conditions between the "vacuum" and the solid[38]). Therefore it seemed appropriate to explore the consequences of using other plausible boundary-value prescriptions for the $Y_{lm}(\hat{k})$. The most obvious of these is the use of the asymptotic external values of k and $k_\perp$. The intensity profiles obtained using this prescription are labeled "Snow-3" in Fig. 1. Substantial differences occur for $E \lesssim 30$ eV between the profiles calculated on both Al(100) and Al(111) using these two boundary conditions, either of which is perhaps defensible since, in both cases, the diffraction *inside* the solid is calculated using the complex k values specified by Eqs. (7). A third plausible boundary condition, motivated by the requirement that the $Y_{lm}(\hat{k})$ for complex k mix the real and imaginary parts of the total partial-wave scattering matrices in the calculation of the cross section in a fashion analogous to this mixing for real k, is that in the final expression for the cross section we take $Y_{lm}^*(\hat{k}') \equiv \bar{Y}_{lm}(\hat{k}')$. Intensity profiles predicted by this external-beam boundary condition are indicated as "Snow-4" in Fig. 1. An extensive series of calculations for Al(100) and Al(111) have

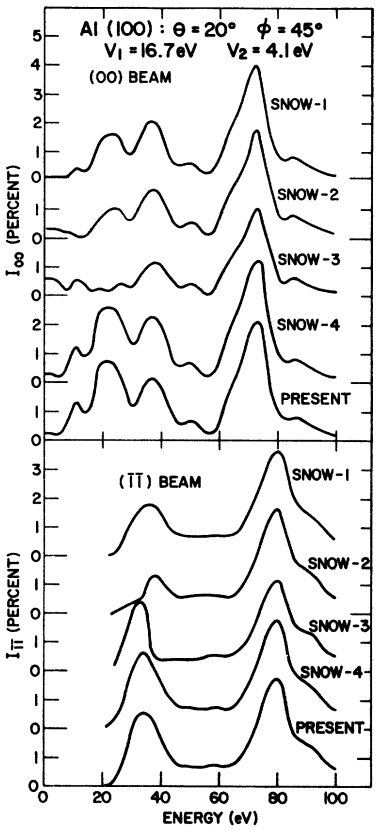

FIG. 1. Intensity profiles for the (00) and $(\bar{1}\,\bar{1})$ beams electrons incident on Al(100) at an angle of incidence of 20° along a ⟨010⟩ azimuth. Our conventions for labeling the azimuthal angles are taken to be those of Jona (Ref. 37). The curves labeled "Snow-1" are calculations of these intensities based on Snow's potential (Ref. 29) as used by Jepsen *et al.* (Ref. 11) performed using the computer program written by Laramore and Duke (Ref. 7). Those labeled "Snow-2" are based on the same potential but performed using a version of the Laramore-Duke program in which complex values of k and $k_\perp$ in the upper-half complex k plane are used consistently to calculate both $Y_{lm}(\hat{k})$ and $Y_{lm}^*(\hat{k})$. [As noted in the text, Laramore and Duke used $-k_\perp'/k$ in calculating $Y_{lm}^*(\hat{k}')$ thereby rendering $-k_\perp'$ a number in the lower-half complex k plane. The profiles labeled "Snow-3" were calculated using the real asymptotic values of k outside the solid in evaluating the $Y_{lm}(\hat{k})$. Those designated as "Snow-4" were obtained using the same $Y_{lm}(\hat{k})$ as in the "Snow-2", but defining $Y_{lm}^*(\hat{k}) \equiv \bar{Y}_{lm}(\hat{k})$ for complex values of k. The set of curves labeled "present" were evaluated using the latter boundary conditions but with the electron–ion-core phase shifts for bulk aluminum predicted by our overlapping-atomic-charge-density model (see Sec. II). All calculations were performed neglecting the thermal motions of the ion cores.

been performed using all three sets of boundary conditions. The use of either the original or the latter two boundary conditions gives generally satisfactory descriptions of Jona's experimental data[37] and a reasonable correspondence with the layer Korringa-Kohn-Rostoker (KKR) method of Jepsen *et al.*[11,15] Since this correspondence is slightly better over all using the "Snow-4" boundary prescription, however, in the figures we show the corresponding intensity profiles (although those predicted by the other boundary conditions were evaluated also).

A second result illustrated in Fig. 1 is the insensitivity of the calculated ELEED intensities to the choice of model potential in the case that the "bulk" potential is used to describe electron scattering from all of the ion cores. The intensity profiles labeled Snow-4 and "present" in Fig. 1 are our model predictions using Snow's self-consistent potential[11,29] and our bulk overlapping-atomic-charge-density potential (see Sec. II). The distinction between the two is barely discernible on the scale of the figure, a result which we found true for a variety of angles of incidence on Al(100). We did not bother to explicitly check this particular result on the other low-index faces because of the extremely small magnitude of the dependence of the ELEED intensities on the bulk potential. It is, however, an important result since it implies that our simple overlapping atomic-charge-density model of the potential may well be adequate for the study of metallic (i.e., small-charge-transfer) chemisorption systems as well as clean metals. Yet it stands in sharp contrast to the conclusions drawn by Pendry[13] from his study of ELEED spectra from the (100) surface of copper. He states that "these spectra are much more sensitive to the details of the ion-core scattering than anticipated" so that a "slight disturbance in the (ion-core scattering) mechanism will produce disproportionately large changes in the spectra."[39] The difference between our results and Pendry's cannot be attributed to the general magnitude of the damping, because Pendry takes $V_2 = 4.0$ eV: almost identical to our value of 4.1 eV. It would be tempting to argue that the discrepancy is caused by the stronger ion-core scattering in Cu. In a series of preliminary calculations, however, Marcus *et al.*[40] find results almost identical to ours for both Al(100) and Cu(100). Moreover, similar results for Ni(100) have been obtained in preliminary calculations by Tong *et al.*[41] Since Pendry does not state the precise prescription which he used to evaluate his "Slater potential,"[42] it is not possible to identify definitively the source of the discrepancy between his conclusions and those of Marcus *et al.*[40] and the present paper. It seems most likely, however, that it resides in his failure to use a muffin-tin model potential to describe the consequences of the overlapping long-range parts of the atomic potentials. It is well known that the Slater exchange approximation fails to give an adequate description of the long-range part of either atomic[30] or crystalline[33] potentials.

Having noted the generally insignificant consequences on calculated ELEED spectra of using different reasonable model potentials to describe the bulk electron–ion-core interaction, we now examine the influence on these spectra of the different surface boundary conditions used by Jepsen *et al.*[11,15,40] and Laramore and Duke,[7,23] respectively. We recall from Ref. 5 and Eqs. (4) that the essential differences in the two boundary conditions involve the treatment of the electron reflection from the solid-vacuum boundary layer itself (whose effects have been discussed elsewhere[5,11]) and the order of the two operations of including an "inner-potential" shift in the energy scale and evaluating the ELEED spectra. Figure 2 illustrates spectra calculated for a net 16.7-eV inner-potential shift inserted into the calculation in three possible ways: *ab initio* ($V_1 = 16.7$ eV), after completion of the calculation ($\Delta = 16.7$ eV), and a mixture of the two ($V_1 = 7.5$ eV, $\Delta = 9.2$ eV). Comparison of the last

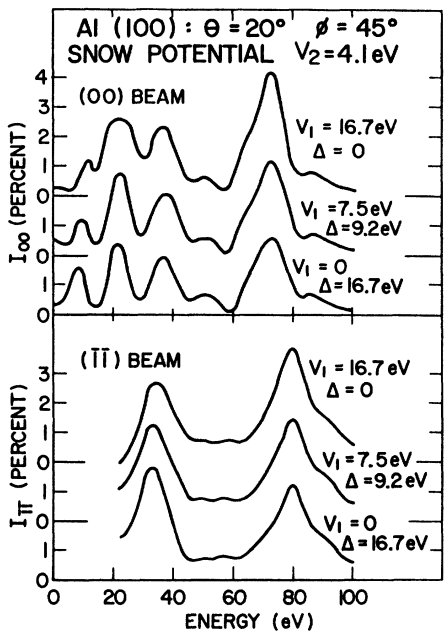

FIG. 2. Intensity profiles for electrons incident on Al(100) at an angle of incidence of 20° along a ⟨010⟩ azimuth. The three profiles for each of the (00) and $(\bar{1}\,\bar{1})$ beams illustrate the consequences of using various combinations of real self-energies and shifts in the energy scale as discussed in association with Eqs. (4) in the text. The electron–ion-core potential used in the calculations is that of Snow (Ref. 29) as applied by Jepsen *et al.* (Ref. 11). The thermal motions of the ion cores were neglected in these computations.

two cases provides a direct comparison of the spectra calculated using the boundary conditions of Laramore and Duke ($V_1 = 7.5$ eV) and of Jepsen *et al.* ($V_1 = 0$) for the value of the inner-potential shift (7.5 eV) used by the latter. The observed differences in the two sets of spectra, while leaving the qualitative appearance of the intensity profiles unaltered, are much larger than those evident either in Fig. 1 or in the analyses of Marcus *et al.*[40] between spectra predicted by different plausible models of the electron–ion-core potential. Moreover, it is significant that these differences persist to quite large energies [because of the influence of the value of V_1 on that of $\mathrm{Im}k(E)$]. For example, the intensity of the maximum at $E = 73$ eV is reduced by 50% when V_1 is taken to be zero and Δ to be 16.7 eV rather than conversely. Thus we see that differences in boundary conditions, which usually are ignored,[5] cause changes in the ELEED spectra which are large relative to those associated with the use of different but sensible bulk electron–ion-core potentials.

We now turn to our final topic in this section: the comparison of our calculations of ELEED intensities with those of Jepsen *et al.*[11,15] Given the sensitivity of the intensities to the boundary conditions, we see that we cannot expect a detailed correspondence between the two of these otherwise identical calculations because of their use of differing vacuum-solid joining conditions[43] and treatments of the thermal motions of the atoms.[44] Nevertheless, a comparison of the predictions of the two models for the specular beam of electrons diffracted from Al(100), Al(110), and Al(111), using $V_1 = 0$, $V_2 = 4.1$ eV, $\Theta_D = 418\,^\circ$K, and Snow's potential as used by Jepsen *et al.*,[11] revealed almost indiscernible differences in the line shapes, for $E \lesssim 70$ eV near normal incidence, but increasing differences even at low energies for increasing angles of incidence. These differences were insensitive to the choice of model potential, as expected from our earlier discussion. At energies $E \gtrsim 70$ eV the two model spectra often differ substantially because of our restriction to three partial waves. A fairly extensive study of the nonspecular beams was undertaken for Al(111) because of the availability of "no-reflection matching" calculations by Jepsen *et al.*[15] for this case. The indexing of the nonspecular beams for the (111) face of fcc metals is indicated in Fig. 3. Typical results (obtained using our overlapping-atomic-charge-density model, however, since the choice of potential proved relatively unimportant) are shown in Fig. 4. Both calculations reproduce the main features of Jona's data rather faithfully with the present results looking noticeably better for some beams [e.g., the (01), $(\bar{1}0)$, and $(1\bar{1})$ beams] and the spectra of Jepsen *et al.* appearing more

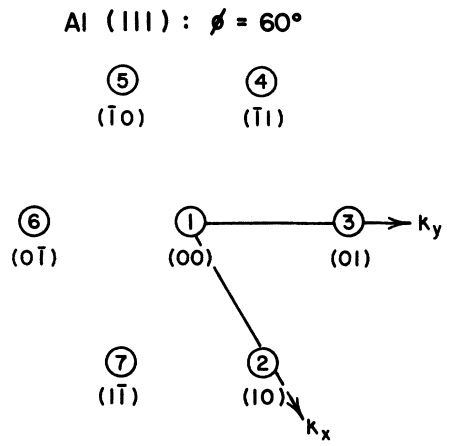

FIG. 3. Schematic diagram of the indexing of the nonspecular beams for an incident beam azimuth of $\phi = 60°$ on Al(111). The numbering of the beams is that of Jepsen *et al.* (Ref. 15) whereas the indexing is due to Jona (Ref. 37).

adequate for others [e.g., the (10) and $(\bar{1}\,\bar{1})$ beams]. The differences between the two calculations near the thresholds for the nonspecular beams is attributed to the differing wave function joining conditions intrinsic to the multiple scattering[7,38] and layer-KKR[11] methods. Small differences in the higher-energy ($E \gtrsim 50$ eV) line shapes easily can be caused by the inclusion of Jepsen *et al.* of more partial waves in their analysis. It should be emphasized, however, that niether calculation reliably reproduces the energies of maxima in the intensities to better than about ± 3 eV.

Finally, the different prescriptions[44] used by Laramore and Duke[7,23,27] and by Jepsen *et al.*[11] to combine the effects of lattice vibrations with those of the rigid-lattice ion-core scattering usually do not create noticeable differences in the isothermal ELEED spectra. The insensitivity of these spectra to the lattice vibration boundary conditions persists, moreover, in the temperature dependences of the spectra predicted by the two methods, respectively. It is customary[23,27,36] to define an effective Debye temperature, $\Theta_D^{\mathrm{eff}}(E_B)$, associated with a prominent peak at energy E_B in the ELEED intensity profiles, in terms of the high-temperature limit, $T \gg \Theta_D$, of Eq. (6b), i.e.,

$$W_\nu(T) \to 3\hbar^2 T / 2M_\nu \kappa (\Theta_D^\nu)^2 . \tag{8a}$$

In this limit, a single scattering model leads to the temperature dependence of the intensity $I(E_B)$ of such a peak being given by

$$d[\ln I(E_B)]/dT = -Y\{[\tilde{k}_\perp(\vec{g}, E) + \tilde{k}_\perp(0, E)]^2 + g^2\}, \tag{8b}$$

$$Y = 3\hbar^2 / M\kappa[\Theta_D^{\mathrm{eff}}(E_B)]^2 . \tag{8c}$$

The quantity M designates the mass of the identical

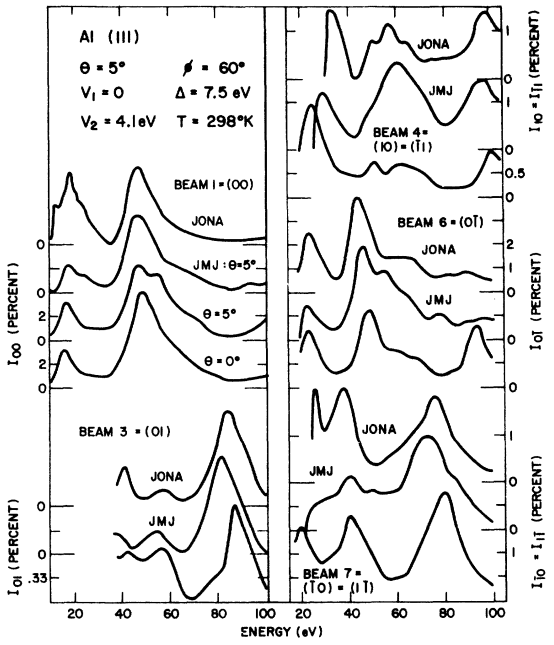

FIG. 4. Intensity profiles for electrons incident on Al(111) at an angle of incidence $\theta = 5°$ along a $\langle 11\bar{2} \rangle$ azimuth. The curves labeled JONA are the experimental data of Jona (Ref. 37) whereas those labeled JMJ are the calculations of Jepsen *et al.* (Ref. 15). The unlabeled curves are our calculations performed using the potential predicted by our overlapping-charge-density model using the local average potential to define the muffin-tin energy zero (i.e., potential 2 described in Sec. II). The phase shifts obtained from this potential are shown in Fig. 7. The models of the inner potential and thermal vibrations were chosen to correspond directly with those used by Jepsen *et al.*, i.e., $V_1 = 0$, $V_2 = 4.1$ eV, $\Delta = 7.5$ eV, and $\Theta_D^{\nu} = 418$ °K for all layers. The intensity scales for our calculations are in percent whereas those for Jona's data and the calculations of Jepsen *et al.* are arbitrary.

atoms on the presumed clean metal surface; $\vec{g}$ is the surface-reciprocal-net vector associated with the scattered beam in which the observed peak (at energy E_B) is found; and $\vec{k}_\perp$ designates an external perpendicular wave vector of an electron [obtained using $\Sigma(E) \equiv 0$ in Eq. (5b)]. Equations (8) provide the requisite definition of $\Theta_D^{\rm eff}(E_B)$ in terms of the predicted temperature dependence of the ELEED spectra. Table III illustrates the values of $\Theta_D^{\rm eff}$ obtained using this definition from ELEED spectra evaluated following the two different prescriptions.[44] Both prescriptions lead to values for $\Theta_D^{\rm eff}(E_B)$ which are identical within the scatter of the calculated intensities. The input Θ_D^{ν} parameters were taken from Laramore's analysis[23] of the temperature dependence of ELEED spectra on Al(100). A discussion of the interpretation of these results is given in Sec. V.

Summarizing, in Sec. III we have examined the sensitivity of our model's predictions of ELEED intensities to input assumptions not specifically associated with surface phenomena. We found that various plausible models of the bulk electron–ion-core potentials all lead to essentially identical ELEED spectra, as do both[7,11] of the common methods of including lattice vibrations into the model. Therefore the predicted intensities are quite insensitive to uncertainties in the description of electron scattering from bulk vibrating ion cores. We discovered, however, a substantial dependence of the predicted low-energy ($E \lesssim 30$ eV) ELEED line shapes on the boundary conditions used to join the wave functions inside and outside the crystal. Moreover, the magnitude of this dependence increases with increasing angle of incidence. Given the uncertainties introduced by the use of differing boundary conditions, our calculations are in quite satisfactory agreement with those of Jepsen *et al.*,[11,15] thereby providing a comforting check on both groups' computer programing.

IV. ELECTRONIC STRUCTURE OF SURFACE ION CORES

We already have seen that the one-electron potential of an ion core depends on its atomic coordination. In Sec. IV we discuss the consequences in the evaluation of ELEED spectra of the altered coordination of ion cores near the low-index surfaces of aluminum as described by our overlapping-atomic-charge-density model. Obviously, other types of surface phenomena, associated with the abrupt termination of the valence-electron charge density, also occur[9] (e.g., surface states and surface-state resonances). We do not discuss these

TABLE III. Values of the effective Debye temperatures $\Theta_E^{\rm eff}(E_B)$, associated with different peaks in the ELEED spectra of normal-incidence electrons diffracted from Al(111). The center column gives the results obtained from the analysis of Ref. 7 and the right-hand column from that of Ref. 11 (Ref. 44). In both calculations $\Theta_D^{\nu=1} = 180$ °K and $\Theta_D^{\nu>1} = 380$ °K were utilized together with the other model parameters used to evaluate the spectra shown in Fig. 4.

Peak energy E_B, and beam index (hk) (units in eV).	$\Theta_D^{\rm eff}$ (°K)	$\Theta_D^{\rm eff}$ (°K)
27.5 (00)	282 ± 10	271 ± 9
57.5 (00)	301 ± 14	300 ± 14
112.5 (00)	432 ± 31	438 ± 30
175 (00)	470 ± 16	472 ± 16
50 $(1\bar{1})$	284 ± 10	286 ± 9
90 $(1\bar{1})$	332 ± 22	331 ± 20
142.5 $(1\bar{1})$	424 ± 24	425 ± 25
37.5 $(0\bar{1})$	190 ± 4	194 ± 4
60 $(0\bar{1})$	246 ± 12	247 ± 11
105 $(0\bar{1})$	373 ± 30	376 ± 31
165 $(0\bar{1})$	432 ± 19	435 ± 20

latter effects here, although they may have some relevance to ELEED for lower incident electron energies[5,14] (e.g., below about 20 eV).

The changes in the electron-ion-core potentials caused by the altered atomic coordination on the Al(100) surface are tabulated in Table II. The associated changes in the ELEED spectra for normally incident electrons are illustrated in Fig. 5. It is apparent from the figure that our two methods (see Sec. II) of computing the bulk electron-ion-core potential from the overlapping-atomic-charge-density model give essentially identical ELEED spectra. Moreover, including a description by either method of the altered electronic structure of surface ion cores creates almost imperceptible alterations in the ELEED intensities. The largest effect occurs in the 52-eV peak as described by method 2. Its energy is reduced by 1 eV and its height augmented by about 10% when the electronic structure of the surface scatterers is incorporated into the model.

Recalling that the potentials at the muffin-tin radius change by as much as 2 eV for the surface scatterers relative to their bulk counterparts, it is informative to examine the associated modifications of the phase shifts. Figures 6 and 7 illustrate these modifications in the case of Al(111). The phase shifts are evaluated for potentials calculated using methods 1 and 2, respectively, as described in Sec. II. The potentials obtained using method 2 are tabulated in Table I. The qualitative features of all the phase-shift-versus-electron-energy curves are identical, although for $E \lesssim 50$-eV differences in detail do occur. For example, it is clear that method 2 predicts substantially enhanced s- and p-wave scattering by the surface ion cores

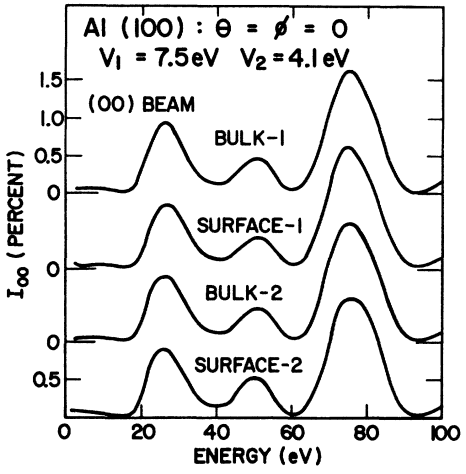

FIG. 5. Intensity profiles for the (00) beam of normally incident electrons elastically diffracted from Al(100). The profiles labeled "Bulk-1" and "Bulk-2" were evaluated using bulk phase shifts obtained from the overlapping-atomic-charge-density model using methods 1 and 2, respectively as described in Sec. II in the text. Those labeled "Surface-1" and "Surface-2" were calculated using phase shifts obtained from this model by following methods 1 and 2, respectively, as defined in Sec. II. The parameters describing the optical potential are noted in the figure. All calculations were performed for a rigid lattice.

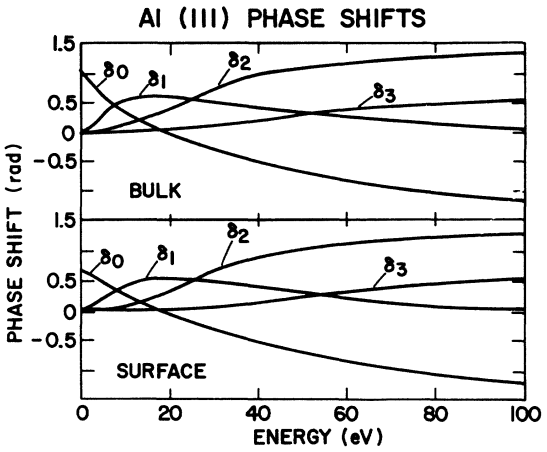

FIG. 6. Phase shifts describing electron scattering from bulk and surface-ion-cores near the (111) face of aluminum. The "bulk" phase shifts describe all ion cores in layers parallel to the surface from the third layer inward. The phase shifts associated with ion cores in the second layer lie between those shown for the top and third layers. These phase shifts were evaluated using method 1 described in Sec. II of the text.

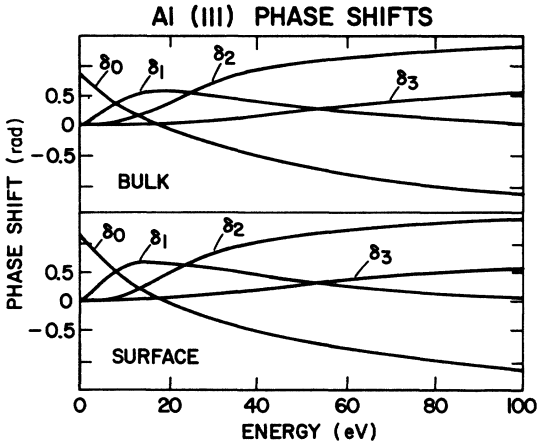

FIG. 7. Phase shifts describing electron scattering from bulk and surface ion cores near the (111) face of aluminum. The "bulk" phase shifts describe all ion cores in layers parallel to the surface from the third layer inward. The phase shifts associated with ion cores in the second layer lie between those shown for the top and third layers. These phase shifts were calculated using method 2 described in Sec. II of the text.

for $E \leq 20$ eV, whereas method 1 predicts reduced scattering in this region. This result is, of course, expected from the construction of the methods because method 1 neglects the changes in the average potential in the flat regions of the muffin tin caused by the reduced surface-atom coordination. The intensity profiles shown in Fig. 4 were calculated using the phase shifts shown in Fig. 7 obtained from the potential tabulated in Table I. All of the phase shifts shown in Figs. 6 and 7 are quite close to the values used by Jepsen *et al.*,[11] although qualitatively different from those of Tong and Rhodin[10] and of Laramore *et al.*[7,12]

Combining the above results with those obtained in Sec. III, we derive two important conclusions. First, changes in the electron–ion-core scattering associated with changes in atomic coordination (*in the absence of charge transfer*) at a solid surface are small and are comparable to those induced by different plausible models of the bulk electron–ion-core potential. Second, alterations in ELEED spectra caused by either of these two sources of changed ion-core scattering are negliglble compared to those caused by different surface boundary conditions for $E \lesssim 100$ eV and by the inclusion of $l \gtrsim 3$ partial waves for $E \gtrsim 70$ eV.

V. SURFACE VIBRATIONAL STRUCTURE

In this section we examine the consequences of the enhanced vibrations of the surface relative to the bulk ion cores. This examination is a necessary prerequisite to our study in Sec. VI of the absolute magnitudes of ELEED intensities since the larger surface-atom motion easily can reduce the calculated intensities by factors of 2–3. Moreover, it is informative to evaluate the consequences on the ELEED line shapes for Al(111) (reported in Sec. III) of the surface vibrational parameters estimated by Laramore[23] in his study of Al(100). Indeed, one of our more interesting findings is an apparent incompatibility between the observed line shapes and temperature dependence of the data of Quinto *et al.*[36] on Al(100), although no analogous incompatibility appears to arise for Al(111). Most of the studies reported in both this section and Sec. VI were motivated by the objective of simultaneously achieving a description of the absolute magnitudes, line shapes, and temperature dependence of measured ELEED spectra from Al(100) and Al(111). [Al(110) was not considered because our hypothesis of a planar surface is thought to be incorrect for existing experimental studies of this surface.[7,15,45]] Even the qualitative achievement of this objective has proven surprisingly elusive.

Upon using our three-phase-shift program with Laramore's Debye-temperature parameters ($\Theta_S \equiv \Theta_D^{\nu=1} = 180\,^\circ$K, $\Theta_D \equiv \Theta_D^{\nu>1} = 380\,^\circ$K), we found immediately that at room temperature, all of the "secondary" structure disappeared. This result is illustrated in Fig. 8. This figure also illustrates that the secondary structure appears both at low temperatures and at room temperature when $\Theta_S = \Theta_D = 380\,^\circ$K. We also verified that it appears at room temperature when both the surface and bulk Debye temperatures are taken to have the surface value $\Theta_D = \Theta_S = 180\,^\circ$K. Consequently, its disappearance appears unique to the high temperature, large-surface-vibration limit that $T > \Theta_S$, $\Theta_S \ll \Theta_D$. Laramore anticipated this result from his analysis

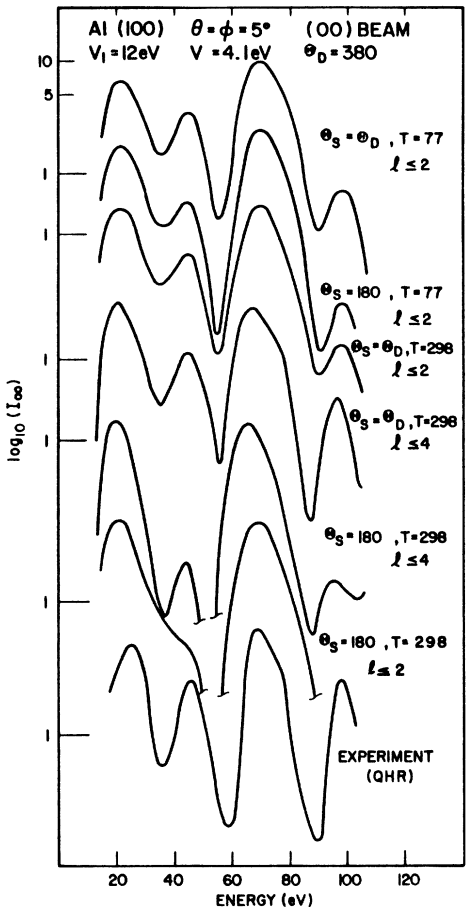

FIG. 8. Intensity profiles for the (00) beam of electrons incident on Al(100) at an angle of incidence of 5° along an azimuth which is 5° off a ⟨010⟩ direction. The upper four profiles are calculated using the potential predicted by our overlapping-atomic-charge-density model evaluated according to method 2 described in Sec. II. The lowest panel illustrates intensities measured at 298°K by Quinto *et al.* (Ref. 36). The optical-potential parameters, effective Debye temperatures, and number of phase shifts (i.e., three for $l \leq 2$ or five for $l \leq 4$) are indicated in the figure. The value of $\Theta_S = 180\,^\circ\text{K} = \Theta_D^{\nu=1}$ is obtained from an analysis of the temperature dependence of the larger peaks in the intensity profile (Ref. 23). The profiles for $l \leq 4$ were calculated by G. E. Laramore of Sandia Laboratories.

of Al(100) based on an isotropic description of the lattice-vibration contributions to the electron–ion-core scattering amplitude.[23] He attributed it to the failure to use five partial waves ($l \leq 4$) in his description of this scattering. In order to examine the sensitivity of the temperature dependence of the profiles to the level of description of the elastic scattering vertex, calculations using five partial waves ($l \leq 4$) were performed, for $\Theta_S = \Theta_D = 380\,^\circ\mathrm{K}$ and $\Theta_S = 180\,^\circ\mathrm{K}$ at room temperature. The results of these calculations also are shown in Fig. 8. They indicate that only a slight improvement in the description of the secondary structure is achieved for $\Theta_S = 180\,^\circ\mathrm{K}$ by including an extra two partial waves in the calculation. Thus, the failure to simultaneously predict the line shapes and temperature dependence of ELEED spectra from Al(100) seems to be related to short-comings of the representation of the temperature dependence of the scattering vertices rather than to limitations of the multiple scattering analysis.

In order to pursue this question further, we decided to undertake a study of the sensitivity of the ELEED spectra from Al(111) to the enhanced vibrations of surface ion cores. Figure 9 illustrates the consequences of a larger value of the imaginary part of the optical potential [as suggested by Laramore's analysis[23] for Al(100)] and of $\Theta_s = \frac{1}{2}\Theta_D$ on the Al(111) ELEED spectra shown in Fig. 4. Evidently, the model's description of the experimental line shapes is, if anything, improved by these alterations in its parameters. While the two changes reduce the absolute intensities by a factor of 2–3 for $E \lesssim 100$ eV, they do not alter substantially the room-temperature line shapes themselves: a sharp contrast to the situation for Al(100). These results augment further our suspicion that the model's failure to describe the room-temperature line shapes for Al(100) may reside in a diffraction phenomenon rather than a technical deficiency of the computer program.

Summarizing, we see that the larger vibrational amplitudes of surface relative to bulk ion cores causes the expected[9] marked influence on the temperature dependence of the ELEED spectra. Less expected is our model's prediction that these enhanced surface vibrations cause major changes in the associated ELEED line shapes for Al(100) but not for Al(111). Once the Θ_D^ν are specified, however, only major (i.e., factor of 2) variations in either the inelastic-collision damping or the electron–ion-core phase shifts can cause substantial (i.e., $\gtrsim 10 - 20\%$) changes in the predicted $\Theta_D^{\mathrm{eff}}(E_B)$. An unfortunate aspect of this relative insensitivity of the temperature dependence to the values of the other model parameters is our failure, thus far, to describe simultaneously the line shape and temperature dependence of the ELEED spectra from Al(100 using a model in which the surface-geometry of this face is taken to be that of a truncated bulk single crystal. This result continues to be valid, moreover, when expansions and contractions of the uppermost layer spacing of up to 10% are incorporated into the model calculations.

VI ABSOLUTE INTENSITIES

The advent of the first measurements[24] of the absolute magnitudes of ELEED intensities from aluminum immediately revealed a puzzle: model calculations which correctly described the observed

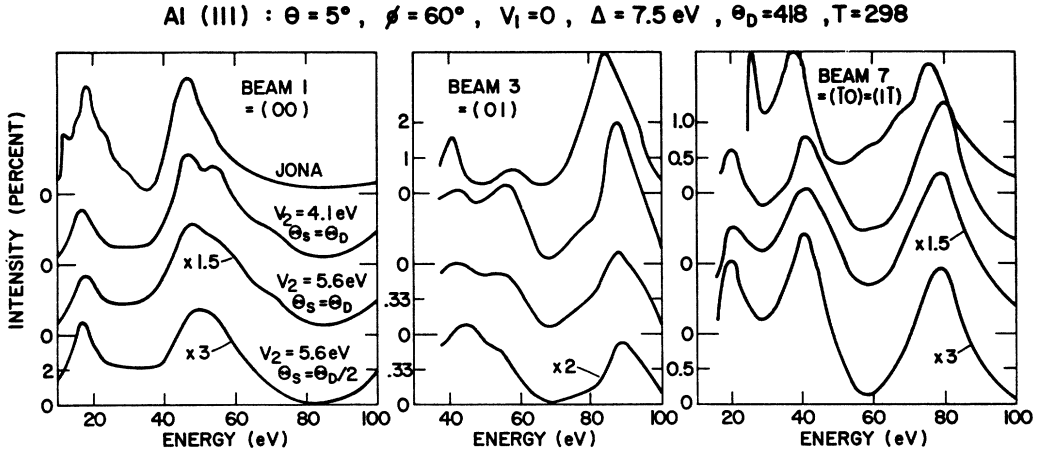

FIG. 9. Intensity profiles for the (00) (left-hand panel), (01) (center panel), and (1 $\bar{1}$) (right-hand panel) beams of electrons scattered from Al(111). The electrons are incident at an angle of 5° along $\langle 11\bar{2} \rangle$ azimuth. All calculations were performed using the overlapping-atomic-charge-density model potential calculated according to method 2 described in the text. $T = 298°$, and the values of V_1, V_2, Δ, $\Theta_S \equiv \Theta_D^{\nu=1}$ and $\Theta_D \equiv \Theta_D^{\nu>1}$ indicated in the figure. The profiles labeled JONA are the experimental data of Jona (Ref. 37).

line shapes predicted absolute intensities about an order of magnitude larger than those observed. In addition, similar although less severe discrepancies have been reported for Cu(100),[11,12] Cu(111),[46] and Ag(111).[46] Since these discrepancies initially motivated the analysis reported in this paper, we conclude by describing the extent to which we have been able to resolve them.

A central feature of the results reported in Secs. IV and V is the failure of specifically surface phenomena to alter the absolute magnitude of ELEED intensities from the low-index faces of aluminum for $E \lesssim 100$ eV by more than a factor of 2–3. Obviously, diffuse scattering caused by surface defects or a disordered surface overlayer could, in principle, account for small ELEED intensities. The reproducibility of the observed intensities from day to day and for various spot positions on the sample[24] argues against this interpretation. If we accept this argument, there remains about an order of magnitude discrepancy between Burkstrand's measured intensities and the present model predictions as well as those of Jepsen *et al.*[11] and of Laramore and Duke.[7]

Since it is well known[25,38] that our model of the optical potential fails to consider specifically surface loss processes (e.g., surface-plasmon emission), and that these processes cause energy losses for electrons outside the solid, it seemed appropriate to investigate the consequences of extending the absorptive optical potential normal to the surface outside the boundary of the surface unit cell. Figure 10 illustrates the results of such a study. The extension of this potential by about one lattice constant beyond the unit cell produces satisfactory qualitative agreement between the calculated and measured absolute intensities, without dramatic modification of the line shape. As shown in Fig. 10, this result is valid for both models of the damping [i.e., Eqs. (3) and (4)], although the uniform absorptive potential, Eq. (4a), tends to suppress the low-energy maxima. Recalling that in self-consistent calculations of the surface barrier, this barrier is predicted to extend beyond the geometrical edge of the solid,[47–49] the corresponding extension of its absorptive component provides a natural and plausible resolution to the intensity puzzle. This suggestion also is in agreement with recent microscopic analyses of the optical potential and effective absorption depth in Auger electron spectra.[25] Consequently, we regard Burkstrand's data as evidence of the importance of surface loss processes on the absolute magnitude of ELEED spectra.

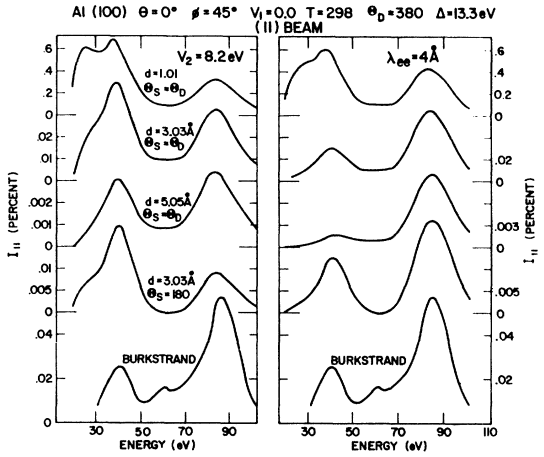

FIG. 10. Intensity profiles for the (11) beam of electrons normally incident on Al(100). The upper four profiles in each panel are calculated using the potential predicted by our overlapping-atom-charge-density model evaluated according to method 2 described in Sec. II. The left-hand panel contains profiles evaluated using Eqs. (4) for the optical potential whereas the right-hand panel contains those calculated from Eq. (3). The parameters used in these optical potentials as well as the vibration parameters $\Theta_S \equiv \Theta_D^{\nu=1}$, $\Theta_D \equiv \Theta_D^{\nu\geq 2}$ are indicated in the figure. The lower intensity profiles labeled "BURKSTRAND" are those measured by Burkstrand (Ref. 24). The notation d designates the depth of the upper layer of ion cores below the position of the onset of the inelastic-collision damping.

VII. SYNOPSIS

In this paper we have examined the role of boundary conditions and specifically surface phenomena in determining the line shapes, temperature dependence, and absolute magnitude of ELEED intensities from Al(100) and Al(111). We found that plausible alterations in the surface matching boundary conditions create larger changes in the ELEED spectra than either different (reasonable) choices of the bulk electron–ion-core potential or modifications of this potential by changes in the atomic coordination of surface ion cores. The enhanced vibrations of surface ion cores, however, exert a strong influence on both the temperature dependence of the ELEED spectra (as is well known from earlier studies[9,23,27,46]) and the "high-temperature" ($T \gtrsim \Theta_S$) line shapes of these spectra. Moreover, specifically surface loss processes, which are responsible for the onset of inelastic-collision damping in front of the geometrical surface of a solid, must be incorporated into the model optical potential in order to describe the absolute magnitude of ELEED intensities from Al(100). Combining all three phenomena into the model leads to a satisfactory description of ELEED from Al(111). The enhanced surface-ion-core vibrations on Al(100) seem to lead to an observed[36] combination of temperature dependence and line shapes of the ELEED spectra, both of which cannot be described simultaneously by our model calculations for either a truncated bulk solid

or one with an expanded (or contracted) surface layer spacing. A possible cause of this failure of the model calculations lies in the limitation of our computer program to a three-phase-shift description of electron–ion-core scattering. The failure is symptomatic, however, of the complicated multiple scattering origin of the smaller maxima in the aluminum ELEED spectra[6,7,22,36] which renders their intensities more sensitive to the model parameters than those of the prominent Bragg maxima.

Finally, it seems appropriate to observe that the study of ELEED from clean aluminum reported herein was undertaken as a preliminary to one of chemisorbed species on fcc metals. Our main concern in this context was the testing of simple models of electron–ion-core potentials and of the description of surface atomic vibrations. From this point of view, the results reported above indicate that in the absence of appreciable charge transfer (e.g., metallic adsorbates on metallic substrates) our overlapping-atomic-charge-density model suffices to provide a sensible estimate of the electron–ion-core potentials even for adsorbed overlayers: an important conclusion because of the simplicity of the model. The analysis of Al(100), however, provides a less encouraging assessment of our Debye model description of the vibrational motion of surface atoms. In particular, it seems that for $T > \Theta_s$ and $\Theta_D > \Theta_s$, the predicted intensity profiles can appear quite different from those calculated at low temperature (i.e., $T \ll \Theta_S$), or for $\Theta_S \equiv \Theta_D$. Although this result could be a consequence of using too few partial waves in our computer program, it also could be caused either by the neglect of phonon emission and reabsorption vertex diagrams in the quantum field theory[27] or by the shortcomings of the Debye model of the atomic vibrations. In any case, however, it seems clear that studies of ELEED line shapes for chemisorption systems are best undertaken at temperatures low relative to the effective Debye temperature of the surface scatterers as determined from the temperature dependence of these line shapes.

ACKNOWLEDGMENTS

The authors are greatly indebted to Dr. G. E. Laramore for providing a copy of his computer program and for his continuing counsel on its construction and modification. The assistance of the Rochester Technical Computer Center in making available large blocks of computer time is gratefully acknowledged. The figures labeled JMJ were taken from a preprint of Ref. 15 graciously provided us by Dr. Jepsen, Dr. Marcus, and Dr. Jona.

[1]J. W. May, Adv. Catal. Relat. Subj. **21**, 151 (1970).
[2]P. J. Estrup and E. G. McRae, Surf. Sci. **25**, 1 (1971).
[3]G. A. Somorjai and H. Farrell, Adv. Chem. Phys. **20**, 215 (1971).
[4]E. N. Sickafus and H. P. Bonzel, Prog. Surf. Membrane Sci. **4**, 115 (1971).
[5]C. B. Duke, in *LEED: Surface Structure of Solids*, edited by L. Laznička (Union of Czechoslovak Mathematicians and Physicists, Prague, 1972), pp. 124–291 and 361–387.
[6]C. B. Duke and C. W. Tucker, Jr., Phys. Rev. Lett. **23**, 1163 (1969); Surf. Sci. **24**, 31 (1971).
[7]G. E. Laramore and C. B. Duke, Phys. Rev. B **5**, 267 (1972).
[8]P. M. Marcus, D. W. Jepsen, and F. Jona, Surf. Sci. **31**, 180 (1972).
[9]See, e.g., C. B. Duke, Annu. Rev. Mater. Sci **1**, 165 (1971) for a review of the considerable literature on this topic.
[10]S. Y. Tong and T. N. Rhodin, Phys. Rev. Lett. **26**, 711 (1971).
[11]D. W. Jepsen, P. M. Marcus, and F. Jona, Phys. Rev. Lett. **26**, 1365 (1971); Phys. Rev. B **5**, 3933 (1972).
[12]G. E. Laramore, C. B. Duke, A. Bagchi, and A. B. Kunz, Phys. Rev. B **4**, 2085 (1971).
[13]J. B. Pendry, J. Phys. C **4**, 2514 (1971).
[14]G. E. Laramore, J. Vac. Sci. Technol. **9**, 625 (1972).
[15]D. W. Jepsen, P. M. Marcus, and F. Jona, Phys. Rev. B **6**, 3684 (1972).
[16]C. B. Duke and C. W. Tucker, Jr., Phys. Rev. B **3**, 3561 (1971).
[17]J. A. Strozier and R. O. Jones, Phys. Rev. Lett. **25**, 516 (1970); Phys. Rev. B **3**, 3228 (1971).
[18]J. B. Pendry, J. Phys. C **4**, 2501 (1971).
[19]C. W. Tucker, Jr. and C. B. Duke, Surf. Sci. **29**, 237 (1972).
[20]C. B. Duke and G. E. Laramore, Surf. Sci. **30**, 659 (1972)
[21]A complete list of references to early analyses of ELEED from the low-index faces of aluminum may be found in Ref. 5.
[22]C. B. Duke, G. E. Larmore, B. W. Holland, and A. M. Gibbons, Surf. Sci. **27**, 523 (1971).
[23]G. E. Laramore, Phys. Rev. B **6**, 1097 (1972).
[24]J. M. Burkstrand, Ph.D. thesis (University of Illinois, 1972) (unpublished); Phys. Rev. B **7**, 3443 (1973).
[25]P. J. Feibelman, C. B. Duke, and A. Bagchi, Phys. Rev. B **5**, 2436 (1972); A. Bagchi and C. B. Duke, Phys. Rev. B **5**, 2784 (1972); P. J. Feibelman, Surface Sci. **36**, 558 (1973).
[26]J. L. Beeby, J. Phys. C **1**, 82 (1968).
[27]C. B. Duke and G. E. Laramore, Phys. Rev. B **2**, 4765 (1970); Phys. Rev. B **2**, 4783 (1970).
[28]C. B. Duke, D. L. Smith, and B. W. Holland, Phys. Rev. B **5**, 3358 (1972).
[29]E. C. Snow, Phys. Rev. **158**, 683 (1967).
[30]F. Herman and S. Skillman, *Atomic Structure Calculations* (Prentice-Hall, Englewood Cliffs, N.J., 1963). Our Eq. (1) is Eq. (1.7) in this reference in which several sign errors have been corrected.
[31]J. C. Slater, Phys. Rev. **81**, 385 (1951).
[32]P. O. Löwdin, Adv. Phys. **5**, 1 (1956).
[33]L. F. Mattheiss, Phys. Rev. **133**, A1399 (1964).
[34]Strictly speaking, we should use a detailed model of the surface-atom dynamics which includes surface as well as bulk lattice vibration modes and anisotropic vibrational amplitudes of the atoms. The effects of the former are described in our model by letting the values of Θ_D^l associated with surface layers be smaller than the bulk values. We neglect the effects of the latter for simplicity. The theoretical background of this model is given in Ref. 27. Recent fairly complete accounts of its application to characterize ELEED data are given by R. J. Reid [Surf. Sci. **29**, 623 (1972)], J. M. Morabito, R. F. Steiger, and G. A. Somorjai [Phys. Rev. **179**, 638 (1969)], and Refs. 3 and 5.

[35]P. A. Flinn and G. M. McManus, Phys. Rev. **132,** 2458 (1963).
[36]D. T. Quinto, B. W. Holland, and W. D. Robertson, Surf. Sci. **32,** 139 (1972).
[37]F. Jona, IBM J. Res. Dev. **14,** 444 (1970).
[38]C. B. Duke and C. W. Tucker, Jr., Surf. Sci. **15,** 231 (1969).
[39]Quoted from just below Fig. 8 in Ref. 13. p. 2522
[40]P. M. Marcus, D. W. Jepsen, and F. Jona, in Proceedings of the Sixth LEED Seminar, 1972 (unpublished).
[41]S. Y. Tong, T. N. Rhodin, and R. H. Tait, in Ref. 40.
[42]See, e.g., Fig. 2 in Ref. 18, Fig. 5 in Ref. 13, and the discussions thereof.
[43]Compare the discussion of Eq. (2.22) in Ref. 7 with that at the end of Sec. II in the second of Refs. 11.
[44]Compare Eqs. (2.31)–(2.36) in Ref. 7 with Eq. (51) in the second of Refs. 11. Although the methods are formally identical, JMJ (Ref 11) use real values of the momenta in evaluating the vertex renormalization, whereas LD (Ref. 7) use the complex values associated with the wave propagation in a dissipative medium.
[45]G. E. Laramore, J. E. Houston, and R. L. Park, J. Vac. Sci. Technol. **10,** 196 (1973).
[46]F. Jona, D. W. Jepsen, and P. M. Marcus, in Ref. 40.
[47]C. B. Duke, J. Vac. Sci. Technol. **6,** 152 (1969).
[48]A. J. Bennett and C. B. Duke, Phys. Rev. **188,** 1060 (1969).
[49]J. A. Appelbaum and D. R. Hamann, Phys. Rev. B **6,** 2166 (1972).